

We are IntechOpen, the world's leading publisher of Open Access books Built by scientists, for scientists

6,900

Open access books available

186,000

International authors and editors

200M

Downloads

Our authors are among the

154

Countries delivered to

TOP 1%

most cited scientists

12.2%

Contributors from top 500 universities



WEB OF SCIENCE™

Selection of our books indexed in the Book Citation Index
in Web of Science™ Core Collection (BKCI)

Interested in publishing with us?
Contact book.department@intechopen.com

Numbers displayed above are based on latest data collected.
For more information visit www.intechopen.com



Arabian Sea Tropical Cyclones: A Spatio-Temporal Analysis in Support of Natural Hazard Risk Appraisal in Oman

Suad Al-Manji, Gordon Mitchell and Amna Al Ruheili

Abstract

Tropical cyclones [TCs] are a common natural hazard that have significantly impacted Oman. Over the period 1881–2019, 41 TC systems made landfall in Oman, each associated with extreme winds, storm surges and significant flash floods, often resulting in loss of life and substantial damage to infrastructure. TCs affect Omani coastal areas from Muscat in the north to Salalah in the south. However, developing a better understanding of the high-risk regions is needed, and is of particular interest in disaster risk reduction institutions in Oman. This study aims to find and map TC tracks and their spatio-temporal distribution to landfall in Oman to identify the high-risk areas. The analysis uses Kernel Density Estimation [KDE] and Linear Direction Mean [LDM] methods to better identify the spatio-temporal distribution of TC tracks and their landfall in Oman. The study reveals clear seasonal and monthly patterns. This knowledge will help to improve disaster planning for the high-risk areas.

Keywords: Oman, Arabian Sea, tropical cyclone, storm track analysis, natural hazard risk assessment, hazard mapping

1. Introduction

Understanding and forecasting the consequences of climate change is critical to support the work of planners and decisions makers. Climate change has touched many aspects of our environment and life; for example, 43% of all natural disasters are related to flooding, which has impacted 56% of all people around the world [1]. Rising global temperature drives more frequent and extreme rainfall events [2], and through thermal expansion, sea level rise. It has been reported that the temperature of the Indian Ocean is increasing faster than other oceans [3]. These factors increase flood risk for coastal zones, particularly those in low lying areas, such as Oman.

These increased risks are expected to persist. For example, in Japan, general circulation models used to forecast the frequency of future storms and cyclones indicate potential losses of about 10 billion USD per year from 100 year return period rainfall events [4]. Similar findings from more frequent and extreme events are projected for central India [5]. Major storms also heavily impact important coastal habitat and ecosystems, particularly coral reefs [6, 7] that are also under climate change pressure from ocean warming and acidification. Recent studies

provide a projection of tropical cyclones (TCs) for 2081–2100 at global and regional scales, and conclude that with a scenario of 2 degrees of global warming, there will be a global reduction in the number of TCs but an increase in TC intensity (more cyclonic events of category 4 and 5), and an increase of tropical cyclonic rainfall amount by 5–20% [8].

These more intense events are often very damaging. For example, the Gulf Coast of the United States was hit by Hurricane Katrina in 2005, resulting in 1300 fatalities, and infrastructure and urban damage costs of \$75 billion. In 2003, Hurricane Isabel struck North Carolina and New Jersey resulting in 40 deaths and \$3.6 billion in damage [9]. The damage risk is exacerbated by urbanization, including in the Gulf countries, as flood hazards are elevated by modification of otherwise natural land surfaces, whilst more people and assets are also exposed to the elevated flood risk [10].

These pressures apply in Oman, where TC's represent a significant risk to people and infrastructure [11]. TCs and storms coming from the Arabian Sea are common in Oman [12, 13]. They are associated with intense rainfall, flash flooding, and can generate tremendous infrastructural, socio-economic and environmental losses [14–16]. For example, TC Gonu, the first category 5 'super cyclone' recorded in the Arabian Sea in a century, hit northern Oman and Iran in 2007, with 78 fatalities, and an estimated \$4.6 billion in damage [12]. Gonu is considered Oman's worst natural disaster but smaller events can be very damaging too; for example a 2002 cyclonic storm (ARB 01) caused about \$50 million in damage [17, 18]. The most intense recent events to impact Oman were in the 2015 North Indian Ocean season, comprising the cyclonic storm Ashobaa and the extreme cyclonic storms Chapala and Megh, both of which resulted in fatalities. Since then southern Oman has experienced flash flooding due to TCs Mekuno and Luban in 2018, with further intense storm events in 2020 [19]. A higher frequency of extreme rainfall events is now considered the new norm in Oman [20].

In the Arabian Sea region, the majority of TCs form near the Laccadive Islands [$\sim 11^\circ$ N, 73° E] in two seasons: the pre-monsoon and the post-monsoon [21]. The pre-monsoon season runs from the end of April to June when the south-west wind rises, and the sea surface becomes very warm. The post-monsoon season runs from September to December, when the south-west wind declines and a northeast wind develop over the Arabian Sea [22].

Recent studies report an increase in the frequency of extremely severe cyclonic storms in the pre-monsoon period [23] an increase attributed to elevated anthropogenic black carbon and sulphate emissions [24]. These anthropogenic emissions lead to a weakening of the climatological vertical wind shear, causing an increase in TC intensity in the Arabian Sea [24].

Most of these more intense TCs make landfall [24] and so pose a growing risk. Understanding cyclone frequency and direction is thus essential in identifying areas at high risk in Oman and supporting disaster management. Therefore, this study analyses TCs in the Arabian Sea to better understand their frequency and direction. The study presents a spatio-temporal analysis of cyclone tracks in the Arabian Sea region, drawing on observations from 1881–2019. The research aims to identify high-frequency seasons, the cyclone direction in each season, and the linear direction trend. The results are intended to identify the more exposed areas around the Arabian Sea, particularly in Oman, and to support disaster risk appraisal and management.

2. Data and methods

A spatial [GIS] database of TCs was created based on tracks obtained from the Indian Metrological Department Atlas for the period 1881–1999 [25, 26] and the

IMD e-Atlas for storm and depression tracks over the North Indian Ocean for 1891–2019 [27]. The data used represent all known major tropical systems in the Arabian Sea, 1881–2019, for which observations are available. The tracks show tropical system intensity [category] with data organized based on the temporal [seasonal and monthly] distribution of cyclone tracks and their point of origin. Tracks that made landfall in Oman were extracted from the total tracks for dedicated analysis.

Two methods were used in the spatio-temporal analysis. First, kernel density estimation [KDE] was used to calculate the TCs density distribution. The standard deviations of the KDE showed the high-density area of tracks and were calculated seasonally and monthly for both total Arabian Sea cyclones, and those making landfall in Oman.

Next, the Linear Direction Mean [LDM] is used to identify the linear trend of tracks [the mean orientation and mean angular direction of cyclone tracks], also by month and season. Adding the temporal dimension is useful as it can reveal seasonal variability in tracks. The LDM statistic is “the angle of a line representing the mean direction or orientation of all the lines in the dataset” [28]. The orientation mean considers only the tracks’ movements, whilst the linear direction mean [θ_R] additionally considers the from/to [e.g. east to west] direction of travel. Esri ArcGIS was used to calculate the LDM and circular statistics of compass angle and circular variance [see below] with tracks defined by each cyclone’s origin and endpoint coordinates plotted in a space graph with origin 0, 0 [28]. The statistics calculated are as follows:

$$Y = \frac{\sum_{i=1}^n \sin \theta_i}{n} \quad (1)$$

$$X = \frac{\sum_{i=1}^n \cos \theta_i}{n} \quad (2)$$

Where X and Y are the rectangular coordinates of the mean point, and n is the number of tracks.

$$OR = \sqrt{X^2 + Y^2} \quad (3)$$

Where OR is the length of the resultant vector [in decimal degree [DD] and subsequently distance, where 1 DD = 111.3 km].

$$\cos \bar{\theta} = \frac{X}{OR} \quad (4)$$

$$\sin \bar{\theta} = \frac{Y}{OR} \quad (5)$$

Where $\cos \bar{\theta}$ is the sum of the cosines of the angles of the track and $\sin \bar{\theta}$ is the sum of the sines of track angles. The mean angular direction θ_R is then:

$$\theta_R = \arctan \left(\frac{\sin \bar{\theta}}{\cos \bar{\theta}} \right) \quad (6)$$

The θ_R of the resultant vector [R] is the mean directional counter clockwise from due east [with a value up to 180°]. The resultant vector [R] shifted into the correct quadrant is the compass angle clockwise from due north [with value 0–360°].

The circular variance [s] shows how much storm track directions deviate from the directional mean, and is analogous to the standard deviation. The circular

variance is calculated from the length of the resultant vector $[OR]$, with the result then subtracted from 1 as [28]:

$$s = 1 - \frac{OR}{n} \quad (7)$$

The circular variance, s , has a value between 0 and 1. If all lines pointed in the same direction, the OR would equal the number of lines n [$OR/n = 1$], and the circular variance [s] = 0. If lines pointed in the opposite direction, then $OR = 0$ and $s = 1$ [28].

The KDE and LDM analyses thus show the location-frequency [density] of the Arabian Sea tropical cyclones [1881–2019] and their mean tracks, and how these factors vary over time, by cyclone intensity, and in particular for those cyclones which pose the most significant risk to Oman, those making landfall.

3. Results

3.1 Arabian Sea tropical cyclones frequency

Table 1 presents summary statistics for TCs that formed in the Arabian Sea, 1881–2019. In total, 236 systems formed in the Arabian Sea; of which 134 made landfall, and 102 died in the Arabian Sea or the Gulf of Aden. India has the highest frequency of Arabian Sea cyclones making landfall, with 26.7% of the total, about half of all those making landfall. Overall 47 systems made landfall in Oman [19.9% of the total], and another 16 entered Omani coastal waters but died at sea [between 60–64° E].

Table 2 shows the monthly distribution of Arabian Sea cyclones. The data is grouped into temporal bands that indicate two to four cyclones occur every 15 years, except for 1955–1984 when twice this rate occurred. There is a high frequency of cyclone formation in May–June and October–November. Half of all landfall events occurred in the pre-monsoon [13 in May, nine in June], and 30% in the post-monsoon [five in September, six in October, plus one in November], a pattern consistent with the shorter record of Membery [29]. Thus the formation of TCs in the Arabian Sea occurs in two distinct seasons; pre-and post-monsoon.

Landfall country	Frequency	%
India	63	26.7
Oman	47	19.9
Pakistan	10	4.2
Somalia	7	3.0
Yemen [Socotra islands]	7	3.0
Terminates at Sea	102	43.2
Arabian Sea	96	40.7
Gulf of Aden	6	2.5
Total	236	100

Source: [IMD archive].

Table 1.
Distribution of tropical systems in the Arabian Sea, 1881–2019.

Years	Jan	Feb	Mar	Apr	May	June	July	Aug	Sep	Oct	Nov	Dec	Total	%
1880–1894	0	0	0	1	2	5	0	0	0	1	3	0	12	5
1895–1909	0	0	0	1	4	5	2	0	0	5	1	1	19	8
1910–1924	0	0	0	1	3	2	0	0	0	2	1	0	9	6
1925–1939	1	0	0	0	5	7	0	0	2	5	4	0	24	9
1940–1954	0	0	0	4	2	6	0	0	1	4	5	1	23	10
1955–1969	0	0	0	0	6	5	3	2	1	5	5	2	29	13
1970–1984	0	0	0	1	6	9	4	0	2	12	10	2	46	21
1985–1999	0	0	0	0	3	6	0	0	1	6	5	3	24	10
2000–2014	0	0	0	0	5	9	0	0	4	6	7	1	32	12
2015–2019	0	0	1	0	2	4	0	0	1	5	1	4	18	6
Total	1	0	1	8	38	58	9	2	12	51	42	14	236	100
%	0%	0%	0%	3%	38%	25%	4%	1%	5%	22%	18%	6%	100	

Source: [IMD archive].

Table 2.
 Monthly distribution of tropical systems in the Arabian Sea, 1881–2019.

3.2 Track analysis of Arabian Sea storms making landfall in Oman

3.2.1 Tracks classification

The tracks analysis (**Figure 1**) reveals a distinct difference in pre-and post-monsoon cyclones. **Figure 1(1)** shows the distribution of cyclone origin point and track in the pre-monsoon by month. All pre-monsoon cyclone origins were in the Arabian Sea, to the south-east in May, moving slightly to the northeast in June, then to the north in July. The tracks vary in each month direction, but a clear pattern of track movement is to the south-west Arabian Sea in May and to the north-west in June and July, although there are numerous cases in June when the track curves northeast toward India.

Figure 1(2) shows the distribution of origin points and tracks in the post-monsoon. Origin points are distributed over a larger area than in the pre-monsoon. Most post-monsoon storms originate in the northeast Arabian Sea in September and move gradually to the south-east and the south Arabian Sea in October–December. However, several storms formed in the Bay of Bengal and track west over India before arriving in the Arabian Sea. The tracks analysis shows that in the post-monsoon, cyclones usually track to the west of the Arabian Sea in September, then gradually to the south-west toward the Gulf of Aden and the Horn of Africa in October–December. However, some November cyclones recurved to India in the east of the Arabian Sea.

The origins and tracks for the sub-set of systems that made landfall in Oman also vary by season and month of formation. **Figure 1(1)** shows pre-monsoon origins and tracks, revealing a distinct difference in tracks within this period. In May, systems frequently travel to the coast between Masirah Island (central Oman) and Salalah in south-west Oman. In June the track direction moves to central to north-east Oman, such that tropical systems arrive at the coast between Masirah Island and Ras Al Had, the easterly most point of Oman at the mouth of the Oman Sea. Note, however, that the historical record indicates that storms occasionally deviate from this general pattern. A strong storm of May 1898 crossed Oman from Ras

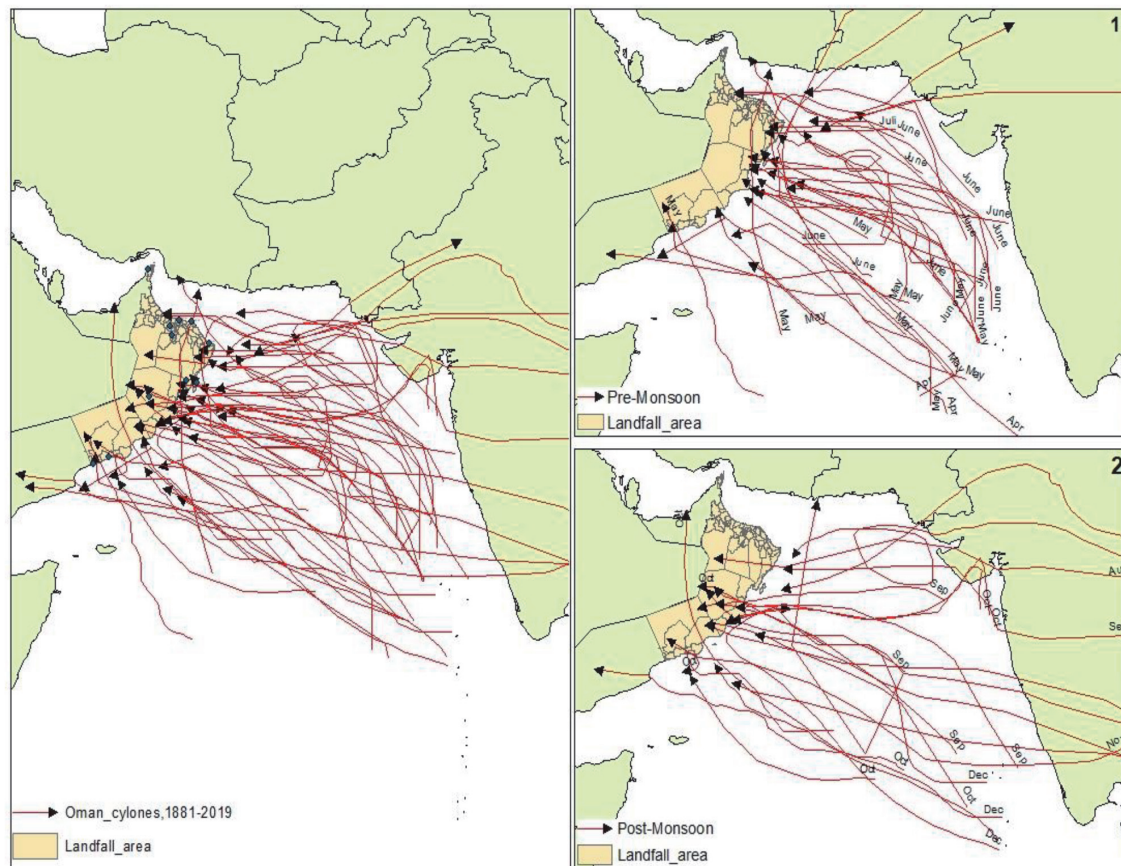


Figure 1. Seasonal distribution of Arabian Sea cyclone tracks with landfall in Oman, 1881–2019: (1) pre-monsoon, (2) post-monsoon.

Madrakah (south of Masirah Island) and moved to north Oman [25], whilst a storm of June 1885 moved to the south-east coast and entered the Gulf of Aden off Yemen [30].

Figure 1(2) shows that the origins and tracks in the post-monsoon similarly have a distinct tracks pattern within this period. In September cyclones track to Central Oman from Masirah Island to Ras Madrakah and then in October–December move progressively toward Salalah in south-East Oman.

3.2.2 KDE of Arabian Sea tracks

Kernel Density Estimation [KDE] is used to analyze cyclone tracks' distribution in the Arabian Sea and identify areas with a high-density of cyclones. **Figure 2** displays the KDE of all tracks in the Arabian Sea and shows a high density of tracks over a large area of the Arabian Sea, from 15–25° N and 60–73° E. In the pre-monsoon (**Figure 2(1)**) there is a high-density of track movement to the north-east, toward the north-west Indian coast (Gujarat), whilst in the post-monsoon (**Figure 2(2)**) the high-density area is more to the south and south-east of the Arabian Sea.

Figure 3 shows the KDE of those tracks that made landfall in Oman. There is a high density of tracks in the mid-East coastline of Oman near Ras Madrakah, which is also evident in the pre-monsoon period (**Figure 3(1)**). In the post-monsoon period, the highest density of tracks is toward the south-east coastline of Oman, near Salalah (**Figure 3(2)**).

Figure 4 shows the KDE of cyclone tracks making landfall in Oman, by pre-and post-monsoon month. In May, the tracks' highest density is in mid-Oman near Ras Madrakah, with some tracks in the south near Salalah. In June there remains a high

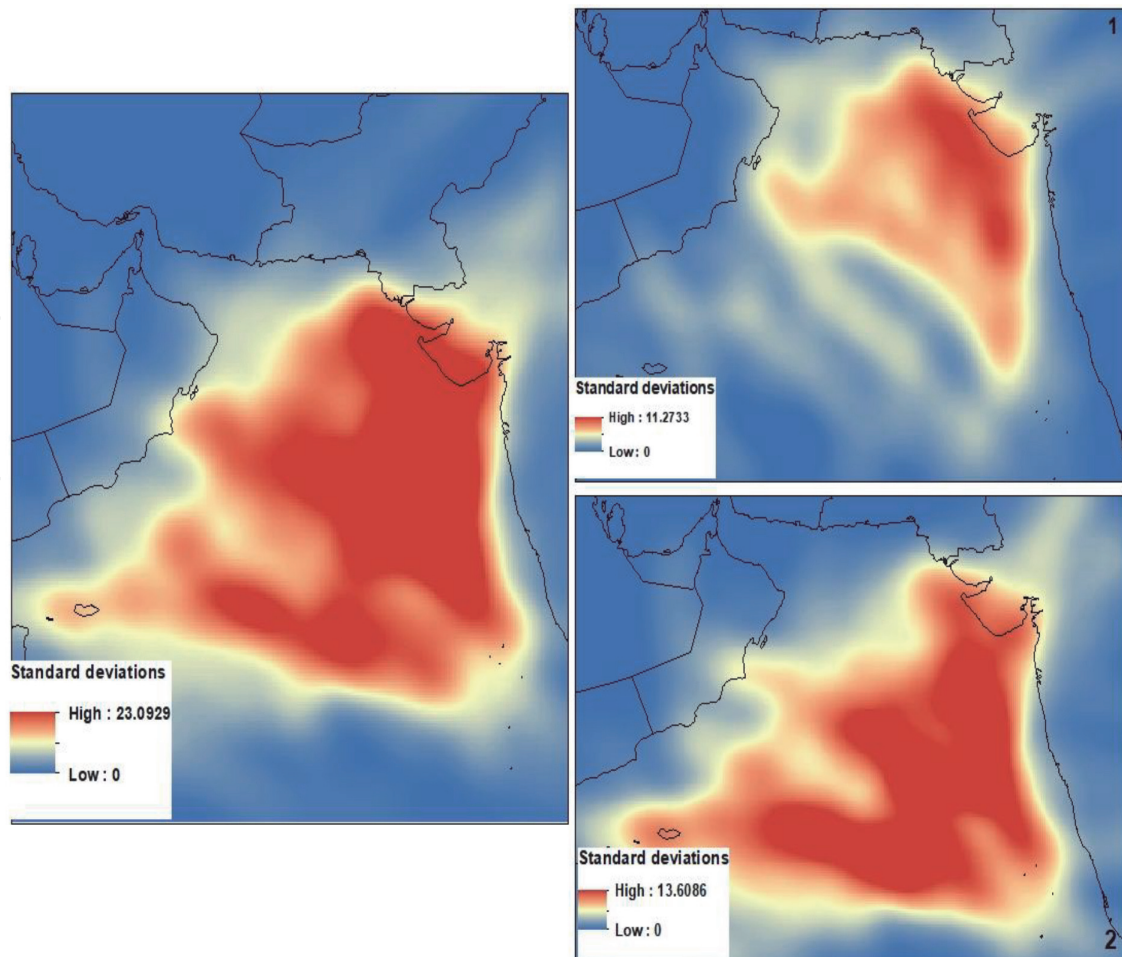


Figure 2.
Kernel density estimation (KDE) of Arabian Sea tracks 1881–2019: (1) pre-monsoon, (2) post-monsoon.

density in mid-Oman, but additionally to the north of Oman, near Ras Al Had. In the post-monsoon, the highest density of the tracks is in mid-Oman near Ras Madrasah in September which moves to the south near Salalah in October.

3.2.3 Linear direction mean of Arabian Sea storm tracks

Linear Direction Mean (LDM) results are presented in **Table 3** and **Figure 5**. For all storm tracks in the Arabian Sea (**Figure 4(1)**) the LDM is to the north-west toward Oman and Iran, with directional mean angle 127.8° (clockwise from due east; compass angle 322.25°), and an average track length of 1480 km. **Figure 4(1)** shows that the LDM in the pre-monsoon is to the north, toward Pakistan, with mean directional angle 120.4° , the post-monsoon LDM is to the north-west toward Oman's north-east coastline, with mean directional angle 136.4° .

Figure 5(1) shows the LDM of those tracks that made landfall in Oman. This track's mean directional angle is 157.8° , to the mid-East Oman coastline south of Masirah Island, and with a mean length of 2169 km. The LDM of the pre-monsoon tracks moved slightly to the north of the LDM of all tracks, to the middle of Masirah Island, with mean directional angle 146.0° , and mean length 1827 km. The post-monsoon landfall tracks have a mean directional angle of 157.9° to Ras Madrasah, with a mean length of 2361 km.

Figure 5(3) shows the LDM of tracks that made landfall in Oman, by seasonal distribution (pre-and post-monsoon), and **Figure 5(4)** shows the monthly LDM of tracks. May and June in the pre-monsoon are the highest frequency storm months.

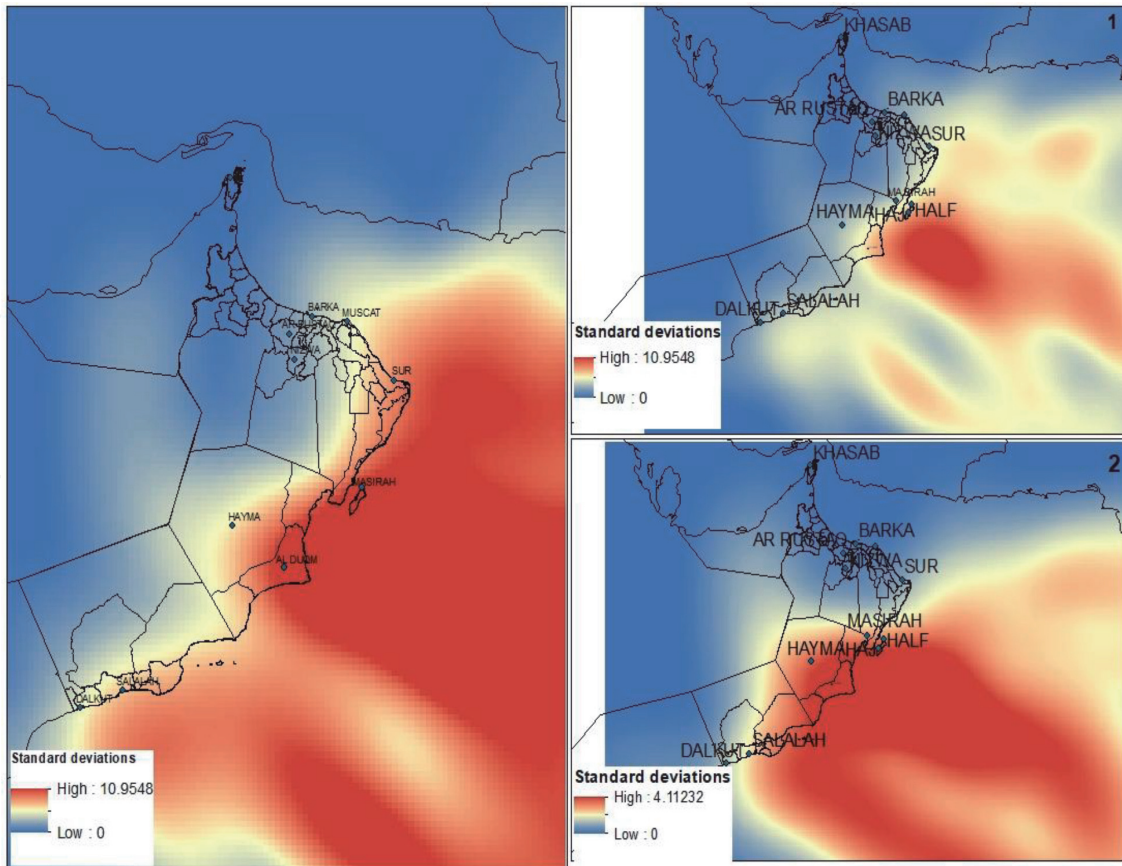


Figure 3. Seasonal kernel density estimation [KDE] of Arabian Sea cyclone tracks 1881–2019, for cyclones making landfall in Oman. (1) pre-monsoon, (2) post-monsoon.

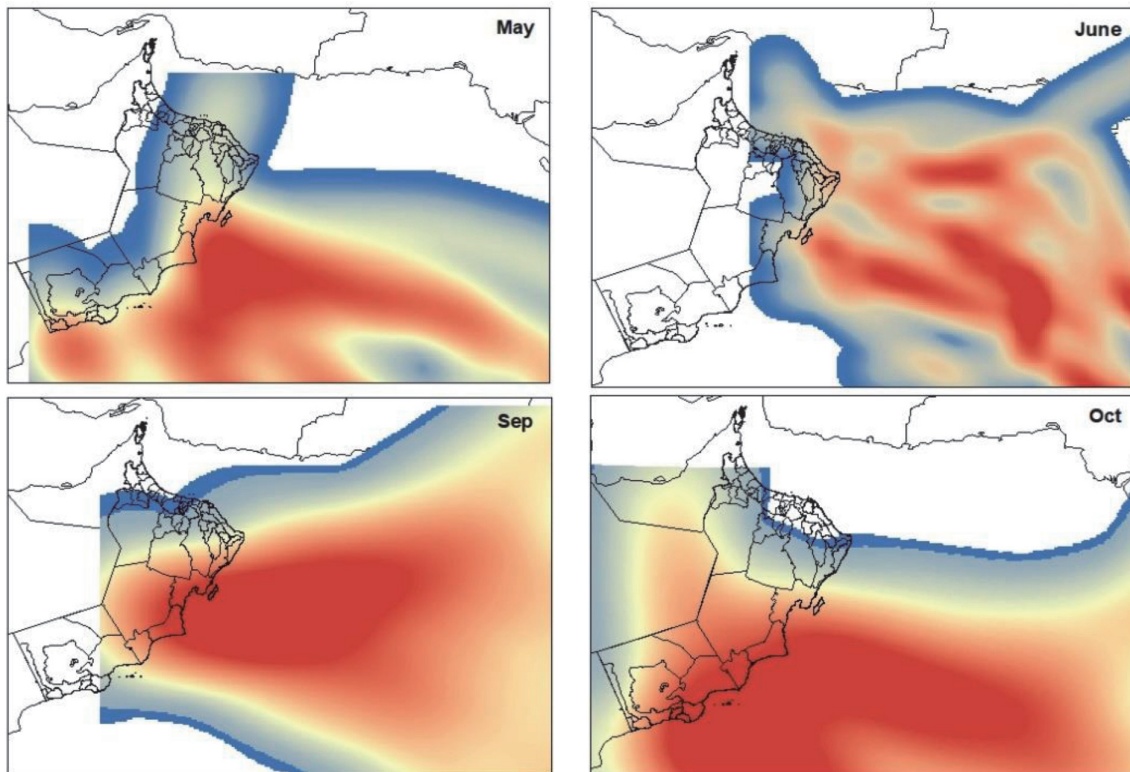


Figure 4. Monthly kernel density estimation [KDE] of Arabian Sea cyclone tracks 1881–2019 for cyclones making landfall in Oman.

Tracks	Compass Angle ¹	Direction Mean angle ² [θ_R]	Circular Variance [s]	X	Y	OR [km]
All tracks	322.25	127.75	0.28	67.72	16.82	1479
Pre-monsoon	332.59	120.41	0.24	67.04	18.96	1221
Post-monsoon	313.63	136.37	0.31	66.27	14.91	1569
Tracks making Oman landfall	298.25	151.75	0.11	64.54	17.09	2169
Pre-Monsoon	302.25	147.74	0.08	63.47	17.11	1827
Post-Monsoon	287.39	162.60	0.03	64.71	2361	
May	302.59	147.41	0.05	62.30	15.71	1748
June	306.30	143.70	0.12	65.35	18.91	1984
Sep	287.63	162.37	0.02	67.99	18.92	2424
Oct	289.22	160.78	0.03	65.87	15.45	2885

Notes. 1. The resultant vector $[R]$ shifted into the correct quadrant clockwise from due north. 2. The directional mean angle $[\theta_R]$ of the resultant vector $[R]$ value up to 180° counter clockwise from due east.

Table 3.
 Linear direction mean (LDM) parameters for Arabian Sea storm tracks, 1881–2019.

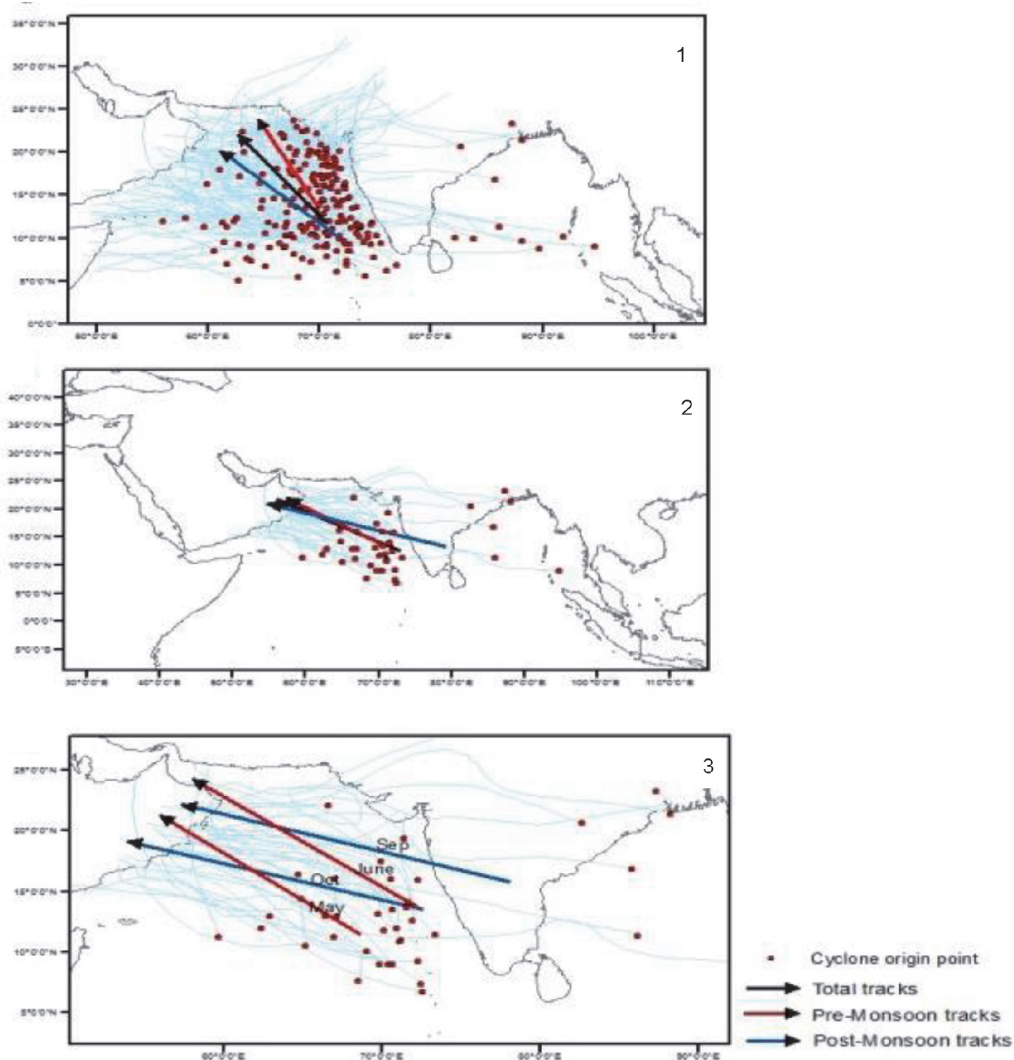


Figure 5.
 Linear direction mean (LDM) of Arabian Sea cyclone tracks: (1) all tracks, (2) tracks making landfall in Oman, and (3) tracks making landfall in Oman by pre- and post-monsoon month.

Storms in May track toward the mid-east coast of Oman and Ras Madrakah. In June storms have a similar LDM but move to the north-west Arabian Sea and toward Oman's capital, Muscat, as they originate further north and east than May storms, whilst having a track length several hundred kilometers greater. A similar situation occurs in the post-monsoon. The LDM of tracks is similar for September and October storms, with October storms originating to the northeast of May storms. September storms thus tend to track toward Masirah Island on Oman's eastern coast, whilst in October, storms making landfall tend to head toward the south-east coast, and Salalah, Oman's main southern city.

4. Discussion

Our study has sought to support the management of risk from natural hazard in Oman, through developing an improved understanding of TC hazard. To do this we have: collated geographical data from the Indian Metrological Department for all known TC and cyclonic storm events in the Arabian Sea since 1881; plotted the tracks of each storm from point of origin to expiration, by storm category (size), by month and season, and with particular reference to those events that made landfall in Oman (these events tend to be large); and conducted a directional analysis to determine likely course of a TC and a spatial (KDE) analysis to determine geographic areas at higher risk of TC makings landfall.

Our analysis sheds light on the origins and tracks of Arabian Sea TCs by season. TCs in the Arabian Sea form in two seasons: the pre-monsoon and the post-monsoon [30, 31]; our analysis reveals a distinct difference in the subsequent TC track between these pre-and post-monsoon periods. All pre-monsoon TCs form in the Arabian Sea itself. In May, they start in the south-east and track to the south-west; in June their origin moves north-east and TCs track north-west; in July TCs form further north still, but continue to track north-west. There are however cases in June when TCs curve north-east toward India. TCs in the post-monsoon period originate over a larger area extending as far as the Bay of Bengal, with TCs tracking west over India to arrive in the Arabian Sea. However, most TCS in this season form in the north-east Arabian Sea in September, then south-east and the south Arabian Sea from October – December. TCs tend to track south-west toward the Gulf of Aden and the Horn of Africa in October–December, although some TCs in the east Arabian Sea recurved to India.

In general, TCs affect Omani coastal areas from Muscat in the north to Salalah in the south (**Figure 6**). Our analysis specifically of those TCs that made landfall in Oman shows that the origins and tracks for systems that make landfall in Oman also vary by season and month of formation. Pre-monsoon TCs tend to originate in the south of the region in May and frequently make landfall between Masirah Island (central Oman) and Salalah in south-west Oman. In June TCs tend to originate further north and make landfall between Masirah Island and Ras Al Had, the easterly most point of Oman at the mouth of the Oman Sea. There are however, some exceptions to this general behavior. Post-monsoon cyclones also have distinct origins and tracks. September TCs tend to form in the north and are likely to make landfall in central Oman, from Masirah Island to Ras Madrakah (Al Duqum), whilst from October–December TCs move progressively toward Salalah in south-east Oman.

Our tracks analysis (part of a wider study of TC resilience in Oman) was first conducted up to and including 2014, and subsequent events have provided an opportunity to test our general conclusions. Early confirmation came from tropical storm Ashobaa in June 2015, which our results suggested would strike Oman in the

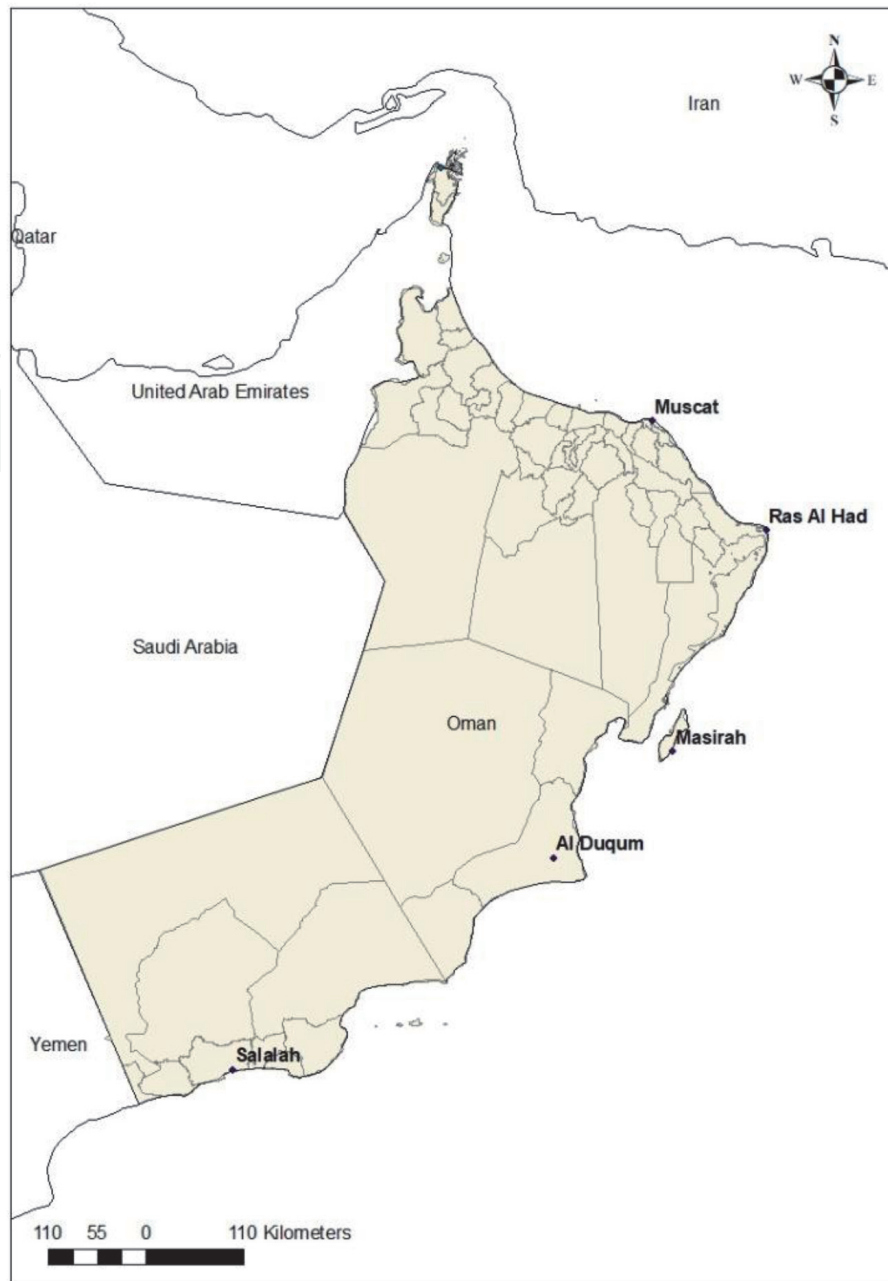


Figure 6.
Oman's coastal areas.

northern region, and indeed this is what happened, with the storm traveling to the north-eastern coast, hitting Oman near Ras-Al Had. Similarly, TC Mukuno that also developed in the pre-monsoon (May 2018), traveled to the south-eastern coast, hitting Salalah and Yemen, as suggested by our analysis. For the post-monsoon we note that TC Hika, which formed in September 2019, traveled to the mid-Omani coastline toward Al Duqum (where it caused substantial damage), whilst TC Luban, formed in the Arabian Sea in October 2018, took a direction to the south-west Arabian Sea toward Salalah and Yemen. Whilst such observations cannot qualify as a formal test of the analysis, they do provide support for the general conclusions as to the seasonal behavior of cyclone tracks in the region.

Thus our analysis reveals a series of general and broadly predictable spatio-temporal patterns. Individual events may deviate from these trends, but the general patterns are useful in informing natural hazard risk assessment and management in the region, including Oman, which has suffered extensive damage in the past due to TCs. The results could, for example, assist with more targeted cyclone preparation

and deployment of emergency response resources, based upon areas most at risk to cyclones overall (strategic planning), and to specific storm events when these are first identified (tactical planning). For example, knowing that cyclones that develop in June are more likely to make landfall in Oman's northern part is valuable emergency planning intelligence.

Globally, the urban area exposed to both flood and drought is forecast to at least double from 2000–2030 [32], indicating the growing importance of understanding and managing these risks. For Oman, the key risk is loss of life and damage from TC. Developing an improved understanding of TC occurrence and behavior, through historical analysis of TC timing and tracks should help to build resilience to TC, and climate change, for the country. Building resilience to TC requires a much wider process of institutional organization and action, which we discuss elsewhere [33] with specific reference to Oman's natural hazard management governance. However, a key element of natural hazard risk management is an understanding of the hazard itself. Our historical analysis of nearly a century and a half of TC tracks in the Arabian Sea, provides enhanced insight into the likely timing and location of TCs making landfall in Oman. This knowledge can support strategic decision making (e.g. prior appraisal of potential flood damage; location prioritization of mitigation resources) and improved understanding of likely destination of TC when they emerge in the Arabian Sea, thus supporting pre-emptive event management.

5. Conclusions

In Oman, tropical cyclones and storms are amongst the most significant natural hazards currently facing the country. Past TCs have resulted in significant loss of life, and billions of dollars in damage costs. The future incidence and behavior of TCs is uncertain, but prediction of a global reduction in TC frequency, but accompanied by an increase in intensity and rainfall when TCs do occur [8], seems to be borne out by recent decades of TC observation in the Arabian Sea region, where fewer but more extreme events are evident.

From our analysis of all recorded Arabian Sea cyclones, we conclude that cyclone tracks vary according to season (pre-and post-monsoon) and month of formation. In the pre-monsoon, cyclones tend to form in the northeast Arabian Sea and moves to the north; in the post-monsoon cyclones tend to form to the southeast Arabian Sea and track to the west.

Whilst there are clearly exceptions evident in the historical record of Arabian TCs spatio-temporal analysis reveals clear seasonal and monthly patterns in the origins and tracks of TCs. This leads to an improved estimation of the likely fate of tropical systems, including a better understanding of where TCs are likely to make landfall in Oman, given their time and point of origin. This knowledge can help improve disaster planning for areas at high-risk.

IntechOpen

Author details

Suad Al-Manji^{1*}, Gordon Mitchell² and Amna Al Ruheili³

1 Ministry of Education, Muscat, Oman,

2 University of Leeds, Leeds, UK

3 Sultan Qaboos University, Muscat, Oman

*Address all correspondence to: suad.almanji@gmail.com

IntechOpen

© 2021 The Author(s). Licensee IntechOpen. This chapter is distributed under the terms of the Creative Commons Attribution License (<http://creativecommons.org/licenses/by/3.0>), which permits unrestricted use, distribution, and reproduction in any medium, provided the original work is properly cited. 

References

- [1] Jonkman, S. N. Global perspectives on loss of human life caused by floods. *Natural Hazards*. 2005; 34[2], 151–175
- [2] Herath, S. M., and Sarukkalige, R. Evaluation of empirical relationships between extreme rainfall and daily maximum temperature in Australia. *Journal of Hydrology*. 2018; 556, 1171–1181
- [3] Roxy, M. K., Ritika, K., Terray, P. and Masson, S. The curious case of Indian Ocean warming. *Journal of Climate*. 2018; 27[22], 8501–8509
- [4] Kazama, S., Sato, A., and Kawagoe, S. Evaluating the cost of flood damage based on changes in extreme rainfall in Japan. *Sustainability Science*. 2009; 4 [1], 61
- [5] Naidu, C. V., Raju, A. D., Satyanarayana, G. C., Kumar, P. V., Chiranjeevi, G., and Suchitra, P. An observational evidence of decrease in Indian summer monsoon rainfall in the recent three decades of global warming era. *Global and Planetary Change*. 2015; 127, 91–102
- [6] Knutson, T. R., McBride, J. L., Chan, J., Emanuel, K., Holland, G., Landsea, C. et al. Tropical cyclones and climate change. *Nature Geoscience*. 2010; 3[3], 157–163
- [7] Cheal, A. J., MacNeil, M. A., Emslie, M. J., and Sweatman, H. The threat to coral reefs from more intense cyclones under climate change. *Global Change Biology*. 2017; 23[4], 1511–1524
- [8] Walsh, K. J., McBride, J. L., Klotzbach, P. J., Balachandran, S., Camargo, S. J., Holland, G. and Sugi, M. Tropical cyclones and climate change. *Wiley Interdisciplinary Reviews: Climate Change*. 2016; 7[1], 65–89
- [9] Bourque, L. B., Siegel, J. M., Kano, M., and Wood, M. M. Weathering the storm: The impact of hurricanes on physical and mental health. *The Annals of the American Academy of Political and Social Science*. 2006; 604[1], 129–151
- [10] Scholz, W., Kaiser, M., and Pallasch, M. The Potentials and Risks of Wadis in Cities in the Gulf Region. In *Handbook of Quality of Life and Sustainability*. 2020; 497–520. Springer, Cham.
- [11] El-Saadawy, O., Gaber, A., Othman, A., Abotalib, A. Z., El Bastawesy, M., and Attwa, M. Modeling Flash Floods and Induced Recharge into Alluvial Aquifers Using Multi-Temporal Remote Sensing and Electrical Resistivity Imaging. *Sustainability*. 2020; 12[23], 10204
- [12] Evan, A. T., and Camargo, S. J. A climatology of Arabian Sea cyclonic storms. *Journal of Climate*. 2011; 24[1], 140–158
- [13] Byju, P., and Kumar, S. P. Physical and biological response of the Arabian Sea to tropical cyclone Phyan and its implications. *Marine Environmental Research*. 2011; 71[5], 325–330.
- [14] Al-Rawas, G. A., and Valeo, C. Relationship between wadi drainage characteristics and peak-flood flows in arid northern Oman. *Hydrological Sciences Journal–Journal des Sciences Hydrologiques*. 2010; 55[3], 377–393
- [15] Al-Qurashi, A., McIntyre, N., Wheeler, H., and Unkrich, C. Application of the Kineros-2 rainfall–runoff model to an arid catchment in Oman. *Journal of Hydrology*. 2008; 355 [1–4], 91–105
- [16] Momani, N. M., and Fadil, A. S. Changing public policy due to Saudi City of Jeddah flood disaster. *Journal of Social Sciences*. 2010; 6[3], 424–428.

- [17] Al Ruheili, A., and Radke, J. Visualisation of 2002 storm surge along the coast of Dhofar, case study of Oman. *Environment, Development and Sustainability*. 2018; 22[1], 501–517
- [18] Al Ruheili, A., Dahm, R., and Radke, J. Wadi flood impact assessment of the 2002 cyclonic storm in Dhofar, Oman under present and future sea level conditions. *Journal of Arid Environments*. 2018; 165, 73–80
- [19] Al Ruheili, A. The Aftermath of Mekuno at Jarziz Watershed in Dhofar. *Modern Environmental Science and Engineering*. 2020; 6[4], 494–499
- [20] Gunawardhana, L. N., Al-Rawas, G. A., and Al-Hadhrami, G. Quantification of the changes in intensity and frequency of hourly extreme rainfall attributed climate change in Oman. *Natural Hazards*. 2018; 92[3], 1649–1664
- [21] Galvin, J. The weather and climate of the tropics: Part 7–Tropical revolving storms, *Weather*. 2008; 63[11], 327–333
- [22] Galvin, J. The weather and climate of the tropics: Part 6–Monsoons, *Weather*. 2008; 63[5], 129–137
- [23] Murakami, H., Vecchi, G. A., and Underwood, S. Increasing frequency of extremely severe cyclonic storms over the Arabian Sea. *Nature Climate Change*. 2017; 7[12], 885
- [24] Evan, A. T., Kossin, J. P., and Ramanathan, V. Arabian Sea tropical cyclones intensified by emissions of black carbon and other aerosols. *Nature*. 2011; 479 [7371], 94
- [25] Indian Metrological Department. Atlas of the Tracks of storms and depressions in the Bay of Bengal and the Arabian Sea 1877–1970. [Internet] 1979. http://www.imdchennai.gov.in/cyclone_eatlas.htm. [Accessed 1st Aug 2020]
- [26] Indian Metrological Department. Atlas of the Tracks of storms and depressions in the Bay of Bengal and the Arabian Sea 1971–1995. [Internet] 1999. http://www.imdchennai.gov.in/cyclone_eatlas.htm. [Accessed 1st Aug 2020]
- [27] Indian Metrological Department. Tracks of storms and depressions in the Bay of Bengal and the Arabian Sea 1971–1995. [Internet] 2019. http://www.imdchennai.gov.in/cyclone_eatlas.htm. [Accessed 1st Aug 2020]
- [28] Mitchell, A. The Esri guide to GIS analysis, volume 2: Spatial measurements and statistics, 1st edn. 2005. Redlands, CA: Esri Press
- [29] Membery, D. Famous for 15 minutes: An investigation into the causes and effects of the tropical storm that struck southern Arabia in June 1996, *Weather*. 1998; 53[4], 102–110
- [30] Membery, D. Monsoon tropical cyclones: Part 2, *Weather*. 2002; 57[7], 246–255
- [31] Membery, D. Monsoon tropical cyclones: Part 1, *Weather*. 2001; 56[12], 431–438
- [32] Güneralp, B., Güneralp, İ., and Liu, Y. Changing global patterns of urban exposure to flood and drought hazards. *Global Environmental Change*. 2015; 31, 217–225
- [33] Al-Manji, S, Lovett, J. and Mitchell, G. Factors affecting disaster resilience in Oman: Integrating Stakeholder Analysis and Fuzzy Cognitive Mapping. *Risk, Hazards and Crisis in Public Policy*. 2021; 12, 1, doi.org/10.1002/rhc3.12201